Chemical Physics 171 (1993) 253–263
North-Holland

tochem. 8 (1978)

Physica Scripta 14

.8.
's. 32 (1960) 1068.

# Stark effect and spectral hole-burning: solvation of organic dyes in polymers

Eric Vauthey [1], Keith Holliday [2], Changjiang Wei [3], Alois Renn and Urs P. Wild
*Physical Chemistry Laboratory, Swiss Federal Institute of Technology, ETH Zentrum, CH-8092 Zürich, Switzerland*

Received 5 October, 1992

Spectral hole-burning studies of nile red and cresyl violet in polyvinylbutyral and polyvinylformal films have been performed. From the shape of spectral holes under the influence of an electric field, the dipole moment difference between the ground and excited state of both dyes has been determined. The Stark effect was investigated at different positions in the inhomogeneously broadened absorption band of the guest molecules. The observed dipole moment difference decreases with increasing wavelength. This variation is caused by the matrix induced dipole moment. For nile red, which is a neutral and polar molecule, the distribution of induced dipole moments is strongly correlated with the orientation of its ground state dipole moment. In the case of cresyl violet perchlorate, which is a salt, this distribution is anisotropic for guests absorbing in the blue part of the inhomogeneous band but becomes more isotropic as the absorption wavelength increases. The wavelength dependence of the observed dipole moment is much stronger and is ascribed to the existence of the cresyl violet perchlorate salt in different states of solvation.

## 1. Introduction

Over the past decade, spectral hole-burning (SHB) has allowed valuable information on the local environment of impurity molecules in solids to be obtained [1–3]. Amorphous hosts provide a large range of sites, causing electronic transition energies to be spread over frequencies $10^3$–$10^6$ times greater than the homogeneous linewidth. Molecules having equal transition energies also correspond to a distribution of different environments, each of which has the same total effect on the transition energy of the guest. These various sets of environments can be probed by burning holes at different wavelengths in the inhomogeneous absorption band.

From such investigations, it is possible to gain insight into solvation processes in liquids. The environment of the guest molecule in a glassy matrix at liquid helium temperatures represents to a great extent the equilibrium solvation of the ground state molecule at the glass transition temperature. On the other hand, this solvent configuration is not the equilibrium solvation which would be reached in a fluid sample in the excited state. In a liquid the solvent can relax very quickly to the new equilibrium configuration.

Besides the electronic energy gap, there are several other properties which are influenced by environment. For example, the linewidth, the dephasing time and the Debye–Waller factor depend on the nature of the host [4,5]. For a given impurity doped matrix, it can be expected that some of the mentioned properties also change from site to site, hence also from one position in the inhomogeneous band to another. A dependence of the hole lifetime and the dephasing rate on the position within the inhomogeneous line has been reported in a crystalline environment, for $Eu^{3+}$ in $KEu(WO_4)_2$ [6]. A dependence of the holewidth on the burning wavelength had previously been observed for a tetraazaporphyrin in Langmuir–Blodgett films [7,8]. Flatscher and Friedrich have reported a variation of the Debye–Waller factor across the absorption band of anthracene in a 2-MTHF glass [9]. Recently, Reul et al. reported a frequency de-

[1] Present address: Institute of Physical Chemistry, University of Fribourg, Pérolles, CH-1700 Fribourg, Switzerland.
[2] Present address: Department of Physics and Applied Physics, University of Strathclyde, Glasgow G4 0NG, UK.
[3] Permanent address: Changchun Institute of Physics, Changchun, People's Republic of China.

pendence of the effect of pressure on the width as well as on the frequency shift of holes burnt in free-base phthalocyanine in polymer matrices [10]. Kador et al. observed an increase of the holewidth and of the matrix induced dipole moment difference between the ground and the excited state from blue to red wavelengths in the centrosymmetric molecule octaethylporphyrin in polystyrene [11]. The variation of the induced dipole moment difference was smaller than expected from an electrostatic model. It was concluded that the frequency shift of the impurity absorption and the inhomogeneous broadening of the absorption band were mainly due to dispersion interaction. A site dependence of the magnitude of the induced dipole moment difference between the ground and the excited state has been observed in tetracene in a benzophenone crystal [12].

In the present paper, a study of the Stark effect on the shape of holes burnt at different wavelengths in the inhomogeneous absorption band of nile red (NR) and cresyl violet (CV) in polyvinylbutyral (PVB) and polyvinylformal (PVF)is described. The hole-burning properties of CV have already been studied [2,13,14]. The molecular dipole moment difference between the ground and the excited state of the CV ion (fig. 2a) has been measured to be 2.1 D in PVB at 615 nm, while the induced dipole moment difference is 0.9 D [13]. NR (fig. 2b) is a non-ionic dye known for its large solvatochromic effect [15], suggesting the dipole moment difference between ground and excited states to be large.

## 2. Stark effect on the shape of a spectral hole

The effect of an electric field on the hole shape has been described in detail previously [16]. Briefly, the hole shape depends on a number of experimental and molecular parameters schematically represented in fig. 1 and listed here:

(i) the dipole moment difference between the ground and the excited state of the free impurity molecule, $\Delta\mu_M$;

(ii) the dipole moment difference induced by the matrix field, $\Delta\mu_i$ (the vector sum of $\Delta\mu_M$ and $\Delta\mu_i$ gives the effective dipole moment difference, $\Delta\mu$);

(iii) the angle, $\theta$, between $\Delta\mu$ and the transition dipole moment, $D$;

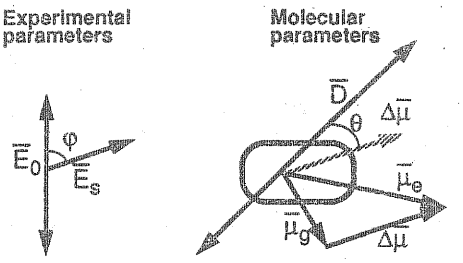


Fig. 1. Schematic representation of the different vectors and angles required to explain the effect of electric field on the shape of a spectral hole. (Symbols given in the text.)

(iv) the angle, $\varphi$, between the applied electric field, $E_S$, and the direction of polarization of the burning light, $E_0$.

In the case of CV, $\theta$ is known to be small [13]. This angle is also expected to be small for NR which has a similar structure to CV. The experimental arrangement allows us to choose $\varphi$ to be 0° or 90°. Molecules with a small angle $\sigma$ between $D$ and $E_0$ are preferentially burned since the absorption probability is proportional to $\cos^2\sigma$. For experiments with $\varphi=0$, these molecules must therefore also have their $\Delta\mu$ vectors mainly parallel or antiparallel to $E_S$ and the maximum interaction with the electric field takes places. The parallel and anti-parallel aligned molecules are spectrally shifted in opposite directions as $E_S$ is varied causing the hole to split. Neglecting the quadratic Stark effect, this splitting, $\Delta\bar{\nu}$, is given by

$$\Delta\bar{\nu}=\frac{2}{hc}\Delta\mu\cdot\mathbf{f}_e\cdot E_S\,, \qquad (1)$$

where $\mathbf{f}_e$ is a tensor describing the relationship between the applied electric field and the resulting change of the local field. This tensor is approximated by the Lorentz field correction, $f_e$ [17]:

$$f_e=(\epsilon+2)/3\,, \qquad (2)$$

where $\epsilon$ is the static dielectric constant of the medium.

When the experimental arrangement is chosen with $\varphi=90°$, the $\Delta\mu$ vectors of the preferentially burned molecules are perpendicular to the electric field and no electrostatic interaction takes place. Molecules which have a $D$ vector not perfectly aligned with $E_0$ may also be burnt and interact subsequently with the Stark field. As a result, the hole is broadened when

the external electric field is changed from the value used during burning [18].

The precise value of $\theta$ can be determined by analysing the hole profile as a function of the Stark field using different experimental geometries.

The effect of the matrix induced dipole moment difference, $\Delta\mu_i$, on the hole shape depends on the distribution of the direction and sizes of the generating local matrix electric fields. In the case of centrosymmetric molecules, this distribution is isotropic and leads to a broadening of the holes upon the application of an external electric field [19,20,21]. In the case of polar molecules, the Stark effect data could be explained with a model consisting of a molecular dipole moment difference, $\Delta\mu_M$, and an isotropically distributed induced dipole moment, $\Delta\mu_i$ [13,16].

In order to extract $\Delta\mu_M$, $\Delta\mu_i$ and $\theta$ from the hole shape, very good signal quality must be achieved as the hole depth becomes very shallow with high electric fields. Holography, which has the advantage of being a zero background method, has proven to be well suited for this type of study [22,23].

## 3. Experimental

PVB and PVF films containing NR (CAS reg. no. 7385-67-3) and CV (CAS reg. no. 41830-80-2) were prepared by the evaporation method [13]. Low temperature absorption spectra and low resolution hole-burning experiments were carried out in an Oxford Instruments CF 1204 helium flow cryostat fitted to a Perkin-Elmer Lambda 9 spectrometer. Fluorescence line narrowing measurements were performed using a total luminescence apparatus which has been described previously [24]. For high resolution hole-burning experiments, the samples were cooled by direct contact with liquid helium in a home-built bath cryostat. Helium was pumped to a pressure of 8 mbar, corresponding to a temperature of 1.6 K. A coherent 699-21 single mode ring dye laser operating with rhodamine 6G or sulforhodamine B was used to burn and probe the holes. The laser frequency was monitored simultaneously by a Tropel 240 spectrum analyser with a free spectral range of 1.5 GHz and a Burleigh WA-10 wavemeter for absolute wavelength calibration. The sample film was inserted between two glass plates and the electric field applied by means of two copper electrodes clamped to the block, perpendicular to the film. The distance between the electrodes was 0.4 cm and the maximum field strength obtained was 2.5 kV/cm. The angle, $\varphi$, between the applied electric field, $E_S$, and the direction of polarization of the burning light, $E_0$, could be changed between 0° and 90° by turning a polarizer. The external electric field was set by a programmable high voltage amplifier providing a voltage range of ±1000 V. The experimental arrangement used for the holographic detection of the holes has been described in detail previously [25].

A Lorentzian lineshape was fitted to the experimental data of the hole to obtain the width and centre frequency. These two parameters and the angle $\theta$ were kept constant during the fit of the theoretical functions [16] to the hole shape measured after the external electric field was applied. A global fit at different values of the electric field was also performed. The angle $\theta$ was determined by fitting the sets of data obtained with both the parallel and perpendicular orientations of $E_S$ and $E_0$. The angle was varied until both fits resulted in the same effective dipole moment difference, $\Delta\mu$.

## 4. Results

The absorption spectra of NR and CV in PVF at 4.2 K are shown in fig. 2 and can be resolved by fluorescence line narrowing [26]. From such measurements the 0–0 band of NR and CV were determined to have their maxima at about 600 and 625 nm with a width (fwhm) of 800 and 600 $cm^{-1}$ [27] respectively. Thus, the maxima of the absorption spectra shown in fig. 2 are dominated by transitions to vibrational excited states. The intensity of the vibronic bands in the absorption spectra of both dyes indicates that the Debye–Waller factors of the two dyes can be expected to be relatively small. This is confirmed by low resolution hole-burning experiments. According to hole shape simulations [28,29], the Debye–Waller factor of NR is about 0.025 in PVF at 4.2 K and at 600 nm. In PVF, using low resolution measurements, the zero phonon line (ZPL) cannot be distinguished from the pseudo-phonon wing, indicating an even smaller Debye–Waller factor. At 1.6 K and with high resolution measurements it was

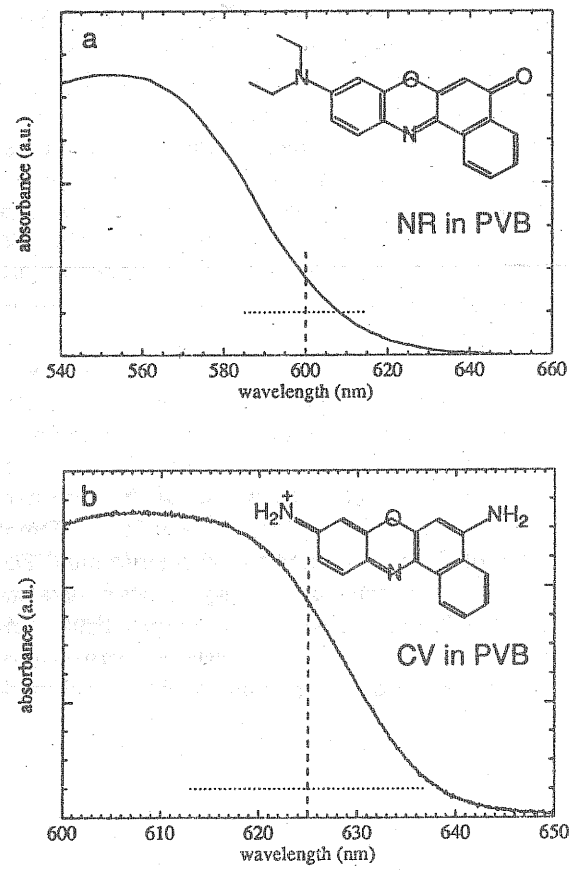


Fig. 2. Absorption spectra of (a) NR and (b) CV in PVB films at 4.2 K. The vertical dashed lines correspond to the centre of the 0–0 transition and the horizontal dotted lines to its inhomogeneous width (fwhm).

sible, although very difficult, to observe the ZPL for NR in PVF. Even with a low burning fluence, the hole became asymmetric due to the presence of the phonon wing on the blue side. For these reasons, the Stark effect on NR in PVF could be measured only at one wavelength. The Debye–Waller factor of CV has been reported to vary from 0.27 to 0.13 depending on the polarity of the host [30].

Fig. 3a shows a surface plot of the diffraction efficiency of a holographically detected hole burned at 600 nm and zero electric field in the NR/PVB system. The electric field, $E_S$, was applied in the direction parallel to the polarization of the light, $E_0$. The data were recorded by stepping the wavelength as successive electric field scans were made. The hole splitting indicates that the angle, $\theta$, between the effective dipole moment difference vector, $\Delta\mu$, and the transition dipole moment, $D$, is relatively small. This is supported by fig. 3b, which shows the effect of applying $E_S$ perpendicular to the polarization of the light. The hole becomes broader as the electric field is increased. When the electric field was returned to zero, the hole width returned to its original zero field value, confirming the absence of irreversible changes.

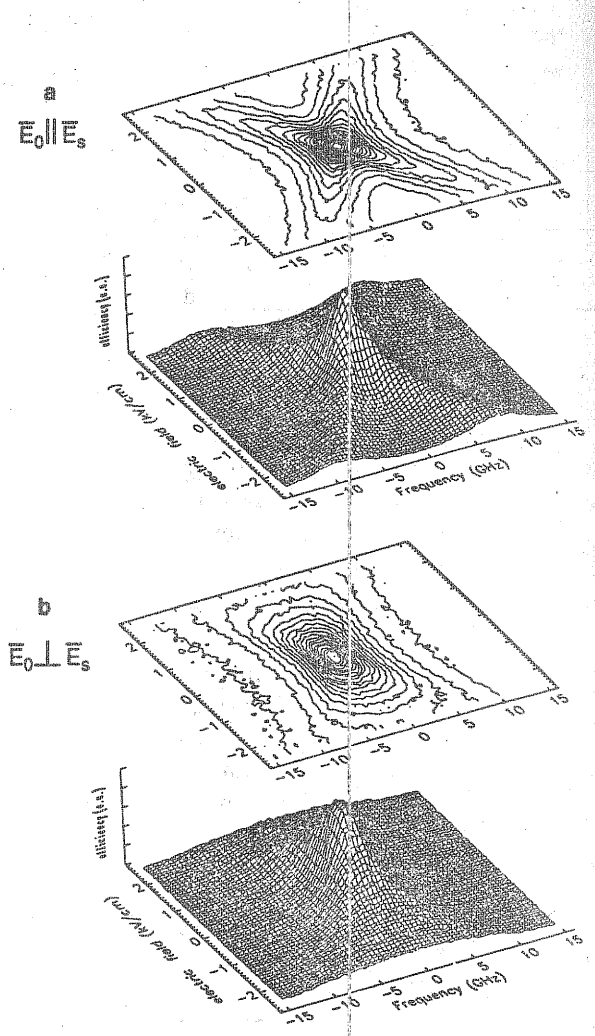


Fig. 3. Electric field dependence of the shape of holes burnt at 600 nm and at zero electric field in NR doped PVB at 1.6 K with the light polarization (a) parallel and (b) perpendicular to the applied electric field.

These measurements were performed at different wavelengths in the absorption band and the values of $\Delta\mu$ and $\theta$ were obtained from the fit. All the data for

Table 1
Wavelength dependence of the effective dipole moment difference of NR in PVB

| Wavelength (nm) | Frequency ($cm^{-1}$) | $\lvert\Delta\mu\rvert$ (D) |
|---|---|---|
| 560 | 17860 | 5.1 |
| 570 | 17540 | 5.1 |
| 580 | 17420 | 5.2 |
| 590 | 16950 | 4.9 |
| 600 | 16670 | 4.7 |
| 605 | 16530 | 4.6 |
| 610 | 16390 | 4.5 |

NR could be fitted with a single variable which describes $\Delta\mu$. At the different wavelengths investigated, the angle $\theta$, for the NR/PVB system, is $29 \pm 3°$ and the effective dipole moment difference, $\Delta\mu$, decreases from the blue to the red as shown in table 1.

The upper limits for the homogeneous linewidth of NR at 1.6 K obtained from the hole width extrapolated to zero power are 1.4 GHz in PVB and about 3.3 GHz in PVF. No significant wavelength dependence of the linewidth was observed. The Stark effect on the NR/PVF system was measured at 600 nm: the angle $\theta$ is the same as in PVB and the dipole moment difference was determined to be smaller than in PVB at the same wavelength (4.1 versus 4.7 D).

In the case of CV in PVB and in PVF, the Stark data are more difficult to interpret. In the blue side of the absorption spectrum, a splitting of the hole (fig. 4a) was observed with the parallel geometry and a broadening with the perpendicular geometry. Nevertheless, both effects are weaker than for NR, indicating a similar value of $\theta$ but a smaller effective dipole moment difference, $\Delta\mu$. The fit could be made satis-

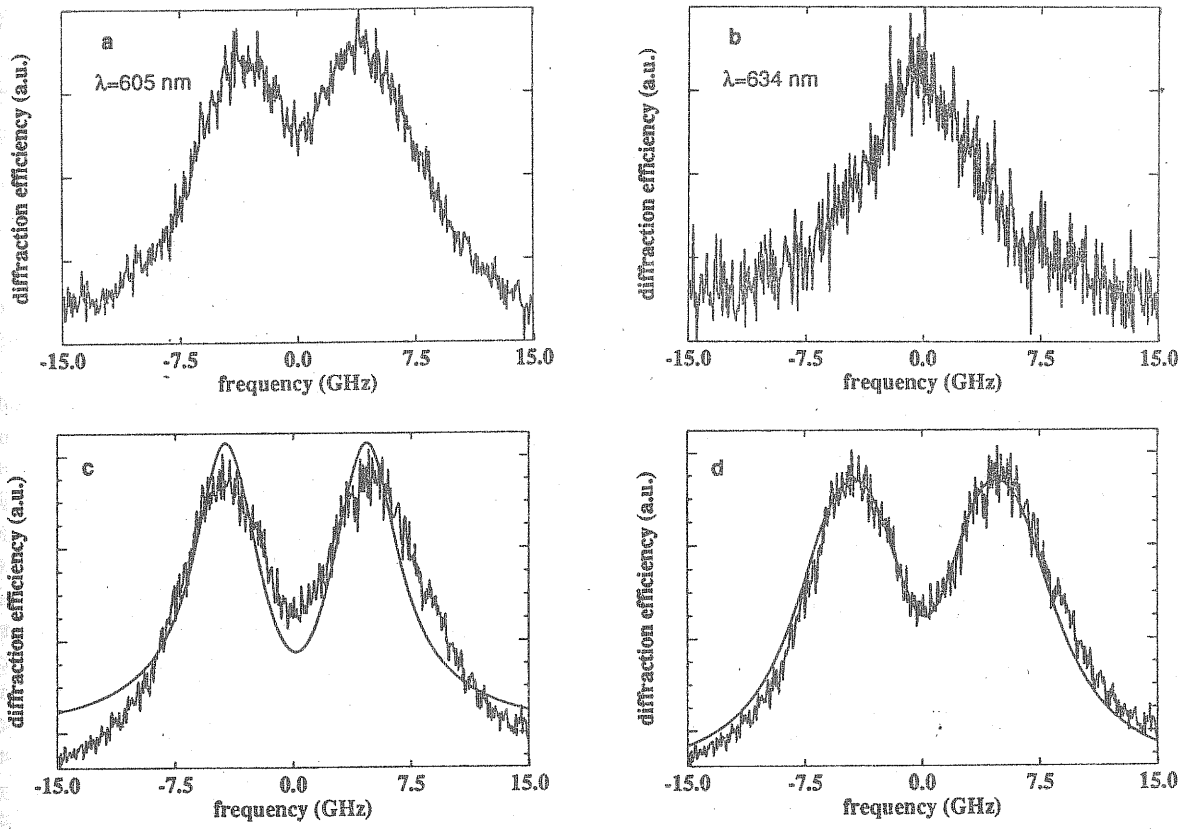


Fig. 4. (a, b): Wavelength dependence of the Stark effect: spectral holes burned in CV/PVF with the parallel geometry at (a) 605 nm and (b) 634 nm at zero electric field and read at 2.5 kV/cm. (c, d): spectral holes burned in CV/PVB with the parallel geometry at 616 nm at zero electric field and read at 1.875 kV/cm, with the best fit obtained (c) without and (d) with the introduction of dipole moment difference vector with a random orientation relative to the molecule.

Table 2
Wavelength dependence of the effective dipole moment difference of CV in PVB using two models: (I) effective dipole moment difference, $|\Delta\mu|$, obtained without considering any isotropic distribution of dipole moment difference; (II) dipole moment differences with a fixed, $|\Delta\mu_{fix}|$, and with a random direction, $|\Delta\mu_{ran}|$, relative to the molecular frame

| Wavelength (nm) | Frequency ($cm^{-1}$) | I | II | |
|---|---|---|---|---|
| | | $\|\Delta\mu\|$ (D) | $\|\Delta\mu_{fix}\|$ (D) | $\|\Delta\mu_{ran}\|$ (D) |
| 593 | 16860 | 3.4 | 3.3 | 1.0 |
| 600 | 16670 | 3.2 | 3.2 | 1.1 |
| 608 | 16450 | 2.9 | 2.9 | 1.1 |
| 616 | 16230 | 2.4 | 2.3 | 1.1 |
| 625 | 16000 | 1.6 | 1.4 | 1.2 |
| 632 | 15820 | 1.2 | 0.7 | 1.2 |

Table 3
Wavelength dependence of the effective dipole moment difference of CV in PVF using two models: (I) effective dipole moment difference, $|\Delta\mu|$, obtained without considering any isotropic distribution of dipole moment difference; (II) dipole moment differences with a fixed, $|\Delta\mu_{fix}|$, and with a random direction, $|\Delta\mu_{ran}|$, relative to the molecular frame

| Wavelength (nm) | Frequency ($cm^{-1}$) | I | II | |
|---|---|---|---|---|
| | | $\|\Delta\mu\|$ (D) | $\|\Delta\mu_{fix}\|$ (D) | $\|\Delta\mu_{ran}\|$ (D) |
| 595 | 16810 | 2.6 | 2.4 | 0.7 |
| 600 | 16670 | 2.5 | 2.5 | 0.7 |
| 605 | 16530 | 2.5 | 2.5 | 0.8 |
| 608 | 16450 | 2.25 | 2.3 | 0.8 |
| 611 | 16370 | 2.1 | 2.2 | 0.9 |
| 616 | 16230 | 1.65 | 1.5 | 0.9 |
| 622 | 16080 | 1.3 | 1.4 | 1.1 |
| 628 | 15920 | 1.0 | 0.9 | 1.4 |
| 634 | 15820 | 0.8 | 0.2 | 1.65 |

factorily with the same procedure as for NR. However, as the burning wavelength increases, the dip between hole components becomes less pronounced than predicted by the theoretical function although the splitting is well reproduced (fig. 4c). Reaching 634 nm, the splitting of the hole can no longer be observed, even with large applied fields (fig. 4b). This broadening can be rationalized by the effect of the matrix induced dipole moment difference whose orientation is not correlated with that of the molecular dipole moment difference. This was then taken into account in the fitting procedure by describing $\Delta\mu$ as the vector sum of a dipole moment difference vector with a fixed direction relative to the molecule, $\Delta\mu_{fix}$, as for NR and a dipole moment difference vector with a random direction, $\Delta\mu_{ran}$. This latter component reflects the effect of a three-dimensional isotropic Gaussian distribution of local fields on the disk-like polarizability tensor of the guest molecule. With this model, the theoretical predictions are in good agreement with the data as demonstrated in fig. 4d. The values obtained from the fit indicate that the angle $\theta$ is $28 \pm 3°$, independent of the wavelength and of the matrix. On the other hand, the values of the dipole moment differences obtained from the fit, $\Delta\mu_{fix}$ and $\Delta\mu_{ran}$, depend on both the wavelength and the matrix (see tables 2 and 3). The values of $\Delta\mu_{fix}$ decrease significantly from the blue to the red wavelengths in both polymers, while the values of $\Delta\mu_{ran}$ increase only slightly in PVB and substantially in PVF.

Finally, the upper limit of the homogeneous linewidth of CV at 1.6 K is 0.6 GHz in PVB [13] and 1.5 GHz in PVF.

## 5. Discussion

The wavelength dependence of the observed dipole moment difference can be understood in terms of an effect of the matrix. The molecular dipole moment difference, $\Delta\mu_M$, is wavelength independent, while the induced dipole moment difference, $\Delta\mu_i$, can have different magnitudes and directions depending on the configuration of the matrix fields around the impurity molecule. This results in a variation of the magnitude and direction of the effective dipole moment difference, $\Delta\mu$, which is observed by Stark effect measurements. Tables 1–3 show that the dipole moment difference vector with a fixed direction, $\Delta\mu_{fix}$, cannot necessarily be interpreted as $\Delta\mu_M$, nor may the dipole moment difference vector with a random direction, $\Delta\mu_{ran}$, be equated completely with $\Delta\mu_i$. This implies that the distribution of $\Delta\mu_i$, hence of the matrix fields, is not isotropic. The relationship between the parameters obtained from the fit and the vectors with a physical relevance for the Stark effect can be summarized with the following equations:

$$\Delta\mu = \Delta\mu_M + \Delta\mu_i = \Delta\mu_{fix} + \Delta\mu_{ran} , \quad (3)$$

$$\Delta\mu_M \neq \Delta\mu_{fix} , \quad (4)$$

$$\Delta\mu_i \neq \Delta\mu_{ran} . \quad (5)$$

Considering the evaporation method used to prepare the samples and the dielectric constants of PVB and PVF ($\epsilon = 3.0$ and 3.4 respectively [31]), it is reasonable to assume that the polymer molecules orientate themselves along the field generated by the impurity molecules in the ground state. In the case of NR, this field originates from its strong ground state dipole, whose magnitude has been estimated to be 7 D [32]. For this reason, the direction of the reaction field is correlated with the orientation of the molecules and the distribution of the induced dipole moments is anisotropic. In other words, the contribution of $\Delta\mu_{ran}$ in eq. (3) is negligible and $\Delta\mu$ is equal to $\Delta\mu_{fix}$.

The magnitude of the induced dipole moment difference, $\Delta\mu_i$, depends on the polarizability difference tensor $\Delta\alpha$ and on the internal electric field, $E_{int}$:

$$\Delta\mu_i = \Delta\alpha\, E_{int} . \quad (6)$$

$E_{int}$ corresponds to the reaction field generated by the matrix:

$$E_{int} = \frac{\mu_g}{a^3} P , \quad (7)$$

where $a$ is the radius of the guest molecule and $P$ a parameter depending on the local polarity of the host. In the present case, only $\Delta\alpha_g$, the component of $\Delta\alpha$ along the ground state dipole moment, $\mu_g$, is relevant. Further, according to a simple electrostatic model [33], the relationship between the frequency shift of the electronic transition energy and the internal field is

$$\bar{\nu} - \bar{\nu}_0 - \Delta\bar{\nu}_{disp} = -\frac{1}{hc}\left[(\Delta\mu_M + \tfrac{1}{2}\Delta\mu_i)\cdot E_{int}\right] , \quad (8)$$

where $\bar{\nu}_0$ and $\bar{\nu}$ are the absorption wavenumbers in the vacuum and in the matrix respectively and $\Delta\bar{\nu}_{disp}$ is the frequency shift due to dispersion interaction. Solvatochromic shift measurements have shown that the absorption band of NR is shifted to the red with increasing solvent polarity. It can therefore be concluded that in PVB and in PVF, the local polarity, hence the internal field experienced by NR, increases from the blue to the red. According to eq. (6), the induced dipole moment difference must follow the same trend. As $|\Delta\mu|$ was observed to decrease from the blue to the red, it can be concluded that $|\Delta\mu| < |\Delta\mu_M|$. The situation is schematically depicted in fig. 5. It can be seen that the decrease of the dipole moment difference of NR with increasing wavelength, that is with increasing internal field, can only be explained by a negative value of $\Delta\alpha_g$, the polarizability difference along the ground state dipole moment.

The value of $\Delta\alpha_g$ can be estimated by combining eqs. (6) and (8):

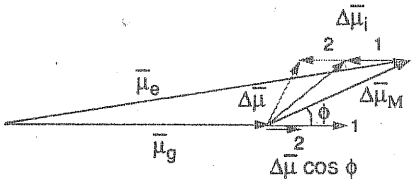


Fig. 5. Schematic representation of the effect of the variation of the magnitude of the induced dipole moment difference, $\Delta\mu_i$, ((1) $\Delta\mu_i$ small, (2) $\Delta\mu_i$ large) on the effective dipole moment difference, $\Delta\mu$, and on its projection along the ground state dipole moment, $\Delta\mu_g$, for NR.

$$\Delta\alpha_g = -\frac{|\Delta\mu_i|^2 + 2|\Delta\mu_i||\Delta\mu_M|\cos\phi}{2hc(\bar{\nu}-\bar{\nu}_0-\Delta\bar{\nu}_{disp})}, \qquad (9)$$

where $\phi$ is the angle between $\Delta\mu_M$ and $\mu_g$. In the present case $\angle$ is parallel to $\mu_g$ as the direction of the reaction f l is assumed to be determined by $\mu_g$ during the sol fication process. The above equation can be arrang to express the relationship between the frequency ift and the resulting variation of the induced dip moment difference:

$$|\Delta\mu_i| = |\ _M|\cos\phi - [(|\Delta\mu_M|\cos\phi)^2 - 2hc\Delta\ (\bar{\nu}-\bar{\nu}_0-\Delta\bar{\nu}_{disp})]^{1/2}. \qquad (10)$$

This eq tion predicts that the wavelength dependence of e induced dipole moment difference should be naller for molecules with large $\Delta\mu_M$, both molecules aving the same polarizability difference. Indeed, f a molecule with a large dipole moment difference small change of the local electric field will result a large frequency shift but will cause only a small v ation of the induced dipole moment difference. s equation has been fit to the measured data usin n angle $\phi$ of 20° (see below) and a value of $2.0\times1$ cm$^{-1}$ as $(\bar{\nu}_0+\Delta\bar{\nu}_{disp})$. This frequency corresponds to the absorption maximum of NR in carbontet chloride which has almost the same refractive i x as PVB and where only dispersion interaction operative. A value for $\Delta\alpha_g/4\pi\epsilon_0$ of $-19$ Å$^3$ and a lecular dipole moment difference, $|\Delta\mu_M|$, of 7.0 D e deduced. Consequently, the magnitude of the exc d state dipole moment is about 15.4 D.

The ne ive value of $\Delta\alpha_g$ does not imply that the average arizability difference, $\Delta\alpha$, is also negative. It is nown that for some aromatic molecules such as itacene, the polarizability difference is positive a ng two molecular axis and negative along the third e, although $\Delta\alpha$ is positive [34]. The large excited s e dipole moment indicates that the electron den y must be more localized than in the ground s e and therefore less polarizable along this direction part from the sign, the magnitude of $\Delta\alpha_g$ is simila o polarizability differences measured or calculate r molecules with a similar structure [35].

Fig. 6 ows $|\Delta\mu|$ measured as a function of frequency f NR. The measured dipole moments can be well r oduced by eq. (9) with the exception of the two ues at the higher frequencies. The Stark

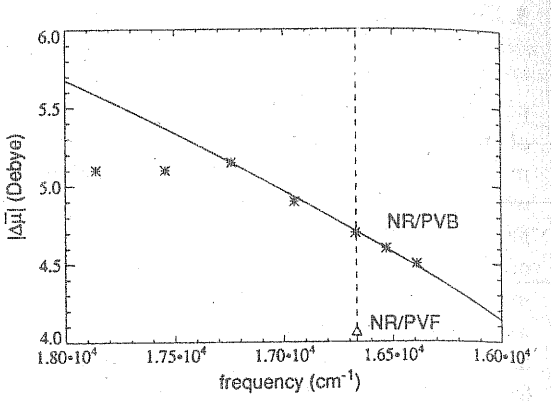


Fig. 6. Frequency dependence of the magnitude of the effective dipole moment difference, $\Delta\mu$, for NR in PVB with the best fit of eq. (10) (full line) and in PVF. (The vertical dashed line corresponds to the centre of the 0–0 transition in PVB.)

effect experiment gives the value of $\Delta\mu$, while the frequency shift depends on the projection of this vector on $\mu_g$. This implies that the relationship between frequency and $\Delta\mu_i$ is correct only if the induced dipole moment distribution *is the same for all sites*. This discrepancy between the observed and calculated dipole moment differences appears at wavelengths which are much shorter than the maximum of the 0–0 inhomogeneous band. Molecules absorbing at these short wavelengths possibly have a different environment and a different distribution of induced dipole moment. This can also explain why the observed dipole moment differences of NR in PVF and PVB are not equal at the same wavelengths as predicted by this simple model.

According to the scheme shown in fig. 5a, the angle $\theta$ should also vary with the wavelength. As the measurements do not show any substantial variation of $\theta$, the angle $\phi$ between $\mu_g$ and $\Delta\mu_M$ must be small.

The dipole moment difference measured from the effect of solvent polarity on the absorption maximum of NR has been reported to be 11.6 D [32]. The discrepancy with our data can have different origins. First, the solvatochromic method can give only an approximate value of the dipole moment difference as the magnitude of various parameters involved in the calculation are difficult to estimate [36]. In particular, the molecular shape is assumed to be a sphere. Second, the nature of the first excited state may depend on the solvent polarity [37]. This can happen for a molecule with two close lying ex-

cited states. In a non-polar solvent, the excited state with the smaller dipole moment difference has the lowest energy while the opposite takes place in polar solvents. Such an effect could lead to a very large solvatochromic effect.

For CV in both PVB and PVF, this simple electrostatic model cannot be applied. The strong wavelength dependence of the hole shape indicates that the induced dipole moment distribution changes substantially throughout the inhomogeneous band. This is further confirmed by the wavelength dependence of the magnitude of both $\Delta\mu_{fix}$ and $\Delta\mu_{ran}$ (see tables 2 and 3). The magnitude of $\Delta\mu_{fix}$ decreases from the blue to the red while the magnitude of $\Delta\mu_{ran}$ increases. This effect indicates that the isotropy of the induced dipole moment distribution increases with decreasing energy, as the direction of $\Delta\mu_i$ becomes less correlated with that of $\mu_g$.

As CV perchlorate is a salt, two extreme cases may be distinguished. First, the salt is not dissociated and the ion pair forms a strong dipole. The distribution of the induced dipole moment would then be anisotropic as for NR, i.e. $\Delta\mu \approx \Delta\mu_{fix}$. Second, the salt is dissociated, the ions are solvated, and the local field corresponds mainly to that generated by a single charge. Therefore, the distribution of the induced dipole moment difference can be expected to be almost isotropic, i.e. $\Delta\mu_i \approx \Delta\mu_{ran}$. Consequently, the observed variation of the Stark effect in CV could be attributed to differing states of solvation of the CV perchlorate salt. The blue part may correspond to CV in the geminate ion pair, while the red part of the absorption band may correspond to solvated free CV cations. In PVF, the isotropy of the induced dipole moment distribution is more pronounced than in PVB. This could be explained by the slightly higher polarity of PVF. In polar solvents, free ions are more stable than geminate ion pairs.

According to solvatochromic shift measurements, the absorption maximum of CV is shifted to the blue as the polarity of the solvent increases. Therefore, the internal field is larger for molecules absorbing in the blue than for those that absorb at longer wavelengths. Fig. 7 shows that the difference between the values of $\Delta\mu$ for CV in PVB and in PVF decreases from the blue to the red frequencies, that is with decreasing internal field. By extrapolation, the gap vanishes below 15600 $cm^{-1}$. At this frequency, the internal field must be zero, and the dipole moment difference corresponds to the molecular dipole moment difference, $\Delta\mu_M$. The data are not precise enough to determine the $\Delta\mu_M$ value, nevertheless it is clearly lower than 1 D. This is smaller than the value of 2.1 D reported in ref. [13]. In that study, $\Delta\mu_M$ was assumed to be identical to $\Delta\mu_{fix}$. As this latter vector contains some contribution from the induced dipole moment difference, its magnitude can be much larger than that of $\Delta\mu_M$.

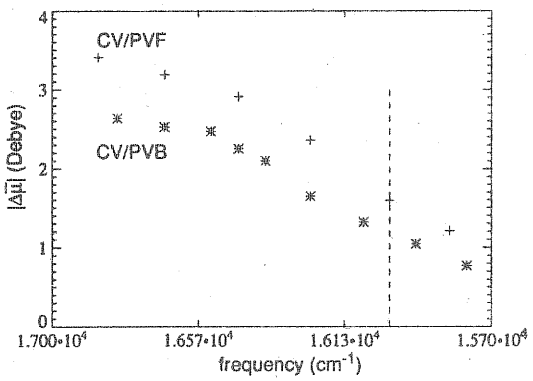


Fig. 7. Frequency dependence of the magnitude of the effective dipole moment difference, $\Delta\mu$, CV in PVB and in PVF. (The vertical dashed line corresponds to the centre of the 0–0 transition in PVB.)

Finally, the measured linewidth at 1.6 K changes strongly from CV to NR and from PVB to PVF. The fluorescence lifetime of NR in PVB is not known but it can be expected to be about 4.5 ns, as measured in tertiary butyl alcohol [38]. This value indicates that the natural linewidth of NR in PVB should be similar to that of CV, of the order of 30 MHz [13]. The increase of the linewidth from CV to NR can possibly be explained by the effect of dipolar coupling to the host [39]. A relationship between the holewidth and the magnitude of the change of dipole moment has been observed for a series of molecules, including CV, in PVB [40]. The measured holewidth of NR in PVB is in agreement with the expected value for a molecule with such a dipole moment difference. Spectral diffusion can also contribute to a further broadening of the holes [41]. For both NR and CV, the linewidth increases from PVB to PVF. This effect could arise from the structure of the polymer. The butyl chain of PVB may result in a packing of the host molecules which is tighter than for PVF [42]. As a con-

sequence the impurity molecules have more freedom to move in PVF than in PVB, causing the dephasing time to decrease and thus the holewidth to increase.

## 6. Conclusion

The wavelength dependence of the Stark effect is a direct manifestation of the amorphous nature of the material. According to the study of Kador et al. [11], the broadening of the homogeneous linewidths of molecules without permanent dipole moments is mainly caused by dispersive interactions. For these molecules, the distribution of the matrix induced dipole moments is isotropic, independent of the wavelength. It is therefore possible to estimate the average polarizability difference between the ground and the excited state from the wavelength dependence of the induced dipole moment. For molecules with large permanent dipoles, electrostatic and polarization interactions also strongly contribute to the inhomogeneous broadening. In this case, the induced dipole moment is due to the reaction field of the matrix. If the induced dipole moment orientation relative to the guest molecule is the same for all sites, its size will be strongly correlated with transition energy. From the wavelength dependence of $\Delta\mu_i$, the projection of the polarizability difference between the ground and the excited state along the direction of $\Delta\mu_i$ can be obtained. The Stark effect for NR in PVB at wavelengths larger than 570 nm can be well described by this model. If the orientation of $\Delta\mu_i$ relative to the molecule, and especially to $\Delta\mu_M$, changes substantially from wavelength to wavelength as observed for CV perchlorate salt in PVB and PVF, this simple correlation between the wavelength and the magnitude of $\Delta\mu_i$ no longer holds. These results show that such studies of the wavelength dependence of the Stark effect can give a better understanding of the origin of inhomogeneous broadening.

## Acknowledgement

We thank Dr. Ross Brown for helpful discussions.

This work was supported by the Swiss National Science Foundation.

## References

[1] W.E. Moerner, ed., Topics in current physics, Vol. 44, Persistent spectral hole-burning: science and applications (Springer, Berlin, 1988).
[2] S. Völker, Relaxation processes in molecular excited states, ed. J. Fünfschilling (Kluwer, Dordrecht, 1989) ch. 3.
[3] K. Hollidy and U.P. Wild, Molecular luminescence spectroscopy – methods and applications, Part 3, ed. S. Schulman (Wiley, New York, 1992) ch. 5.
[4] H.P. Thijsen, R. Van den Berg and S. Völker, Chem. Phys. Letters 97 (1983) 295.
[5] D. Haarer, J. Luminescence 18/19 (1979) 453.
[6] N.B. Man and P.T.H. Fisk, J. Luminescence 45 (1990) 429.
[7] J. Bernard, M. Orrit, R.I. Personov and A.D. Samoilenko, Chem. Ph. Letters 164 (1989) 377.
[8] Y. Romanovskii, R.I. Personov, A.D. Samoilenko, K. Holliday and U.P. Wild, Chem. Phys. Letters 197 (1992) 373.
[9] G. Flatsch and J. Friedrich, Chem. Phys. Letters 50 (1977) 32.
[10] S. Reuf, W. Richter and D. Haarer, Chem. Phys. Letters 180 (1991) 1.
[11] L. Kador, Jahn, D. Haarer and R. Silbey, Phys. Rev. B 41 (1990) 12 15.
[12] A.P. Marc tti and M. Scozzafava, Mol. Cryst. Liq. Cryst. 31 (1975) 15.
[13] A. Renn, S. E. Bucher, A.J. Meixner, E.C. Meister and U.P. Wild, J. Li minescence 39 (1988) 181.
[14] L. Shu an G.J. Small, J. Opt. Soc. Am. B 9 (1992) 724.
[15] J.F. Deye, .A. Berger and A.G. Anderson, Anal. Chem. 62 (1990) 61 .
[16] A.J. Meixr r, A. Renn, S.E. Bucher and U.P. Wild, J. Phys. Chem. 90 1986) 6777.
[17] C.J.F. Bö cher and P. Bordewijk, Theory of electric polarizati (Elsevier, Amsterdam, 1978).
[18] K. Hollida , E. Vauthey, M. Croci, A. Renn and U.P. Wild, J. Opt. So Am. B 9 (1992) 982.
[19] V.D. Sam lenko, N.V. Razumova and R.I. Personov, Opt. Spectry. 5 (1982) 346.
[20] U. Bogner P. Schätz, R. Seel and M. Maier, Chem. Phys. Letters 10 (1983) 267.
[21] L. Kador, . Haarer and R.I. Personov, J. Chem. Phys. 86 (1987) 53 0.
[22] U.P. Wild S.E. Bucher and F.A. Burkhalter, Appl. Opt. 24 (1985) 15 6.
[23] A. Renn, .J. Meixner, U.P. Wild and F.A. Burkhalter, Chem. Ph . 93 (1985) 157.
[24] J.W. Hofst aat, R. Locher and U.P. Wild, Appl. Spectry. 44 (1990) 13 7.
[25] A.J. Meixne (1989) 672
[26] A.J. Kallir, and U.P. Wi
[27] S.E. Bucher,
[28] J. Friedrich, (1980) 705.
[29] I. Lee, J.M. 3463.
[30] R. Van den 257.
[31] Encyclopedi 2nd Ed. (Wi
[32] D. Reiser an 86 (1982) 1

[25] A.J. Meixner, A. Renn and U.P. Wild, J. Chem. Phys. 91 (1989) 6728.
[26] A.J. Kallir, G.W. Suter, S.E. Bucher, E. Meister, M. Lüönd and U.P. Wild, Acta Phys. Pol. A 71 (1987) 755.
[27] S.E. Bucher, Thesis 8541, Zürich (1988).
[28] J. Friedrich, J.D. Swalen and D. Haarer, J. Chem. Phys. 73 (1980) 705.
[29] I. Lee, J.M. Hayes and G.J. Small, J. Chem. Phys. 91 (1989) 3463.
[30] R. Van den Berg and S. Völker, Chem. Phys. 128 (1988) 257.
[31] Encyclopedia of polymer sciences and engineering, Vol. 17, 2nd Ed. (Wiley, New York, 1989).
[32] D. Reiser and A. Laubereau, Ber. Bunsenges. Phys. Chem. 86 (1982) 1106.
[33] N. Mataga and T. Kubota, Molecular interactions and electronic structure (Dekker, New York, 1970).
[34] J.H. Meyling, W.H. Hessenlink and D.A. Wiersma, Chem. Phys. 17 (1976) 353.
[35] I. Renge, J. Opt. Soc. Am. B 9 (1992) 719.
[36] P. Suppan, J. Photochem. Photobiol. A 50 (1990) 293.
[37] P. Jacques, J. Phys. Chem. 90 (1986) 5535.
[38] G.B. Dutt, S. Doraiswamy and N.J. Periasamy, Chem. Phys. 92 (1991) 5360.
[39] R. Silbey and K. Kassner, J. Luminescence 36 (1987) 283.
[40] C. De Caro, A. Renn, U.P. Wild and L.W. Johnson, J. Luminescence 50 (1991) 309.
[41] L.R. Narasimhan, K.A. Littau, D.W. Pack, Y.S. Elschner and M.D. Fayer, Chem. Rev. 90 (1990) 439.
[42] H.P.H. Thijssen and S. Völker, Chem. Phys. Letters 120 (1985) 496.